

Zero-temperature study of a tetrameric spin-1/2 chain in a transverse magnetic field

Javad Vahedi^{1*}, Mahboubeh Shabani Arbousara², Saeed Mahdavifar²

¹*Department of Physics, Sari Branch, Islamic Azad University, Sari, Iran.*

²*Department of Physics, University of Guilan, 41335-1914, Rasht, Iran.*

(Dated: January 27, 2023)

We consider an alternating Heisenberg spin-1/2 antiferromagnetic-ferromagnetic ($AF - F$) chain with the space modulated dominant antiferromagnetic exchange and anisotropic ferromagnetic coupling (tetrameric spin-1/2 chain). The zero-temperature effect of a symmetry breaking transverse magnetic field on the model is studied numerically. It is found that the anisotropy effect on the ferromagnetic coupling induces two new gapped phases. We identified their orderings as a kind of the stripe-antiferromagnetic phase. As a result, the magnetic phase diagram of the tetrameric chain shows five gapped quantum phases and the system is characterized by four critical fields which mark quantum phase transitions in the ground state of the system with the changing transverse magnetic field. We have also exploited the well known bipartite entanglement (name as concurrence) and global entanglement tools to verify the occurrence of quantum phase transitions and the corresponding critical points.

PACS numbers: 75.10.Pq, 75.10.Hk

I. INTRODUCTION

At zero temperature, quantum fluctuations play the dominant role and with the ground state properties the physics of a system determined. The quantum fluctuations cause a fundamental change in the state of a system which is known as the quantum phase transition¹. The one-dimensional (1D) bond alternating Heisenberg spin-1/2 models which are obtained by a space modulation in the exchange couplings represent one particular subclass of low-dimensional quantum magnets which pose interesting theoretical²⁻¹⁸ and experimental¹⁹⁻²⁹ problems. There is a spin-gap in the excitation spectrum of the bond alternating spin-1/2 chains. The mentioned spin-gap causes a plateau shape in the curve of the response functions specially the magnetization.

The study of the induced effects of the space modulation on the exchange couplings has attracted much interest in recent years³⁰⁻⁴¹. It is known that the magnetization curve of a trimerized Ferromagnetic-Ferromagnetic-Antiferromagnetic Heisenberg spin-1/2 chain shows a plateau at 1/3 of the saturation^{30-32,36} but in a Ferromagnetic-Antiferromagnetic-Antiferromagnetic chain a mid-plateau is reported^{35,36}. Another kind of the alternating chains is known as the tetrameric chain^{33-35,37,38}. In this model a mid-plateau is also appeared in the magnetization curve by applying an external magnetic field.

Here, we continue the study of the zero temperature physics of the tetrameric spin-1/2 Heisenberg chains (see Fig. 1). The tetrameric model is defined as an alternating Heisenberg $AF - F$ chain with the space-modulated

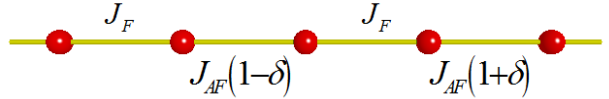


FIG. 1: (Color online.) The schematic picture of alternating tetrameric spin-1/2 chain.

antiferromagnetic exchange³⁸. The Hamiltonian of the model is written as

$$H = -J_F \sum_{j=1}^{N/2} [S_{2j}^x S_{2j+1}^x + S_{2j}^y S_{2j+1}^y + \Delta S_{2j}^z S_{2j+1}^z] + J_{AF} \sum_{j=1}^{N/2} [1 + (-1)^j \delta] \mathbf{S}_{2j-1} \cdot \mathbf{S}_{2j} - h \sum_{j=1}^N S_j^x, \quad (1)$$

where S_j is the spin-1/2 operator on the j -th site. J_F and $J_{AF}^\pm = J_{AF}(1 \pm \delta)$ denote the ferromagnetic and antiferromagnetic couplings respectively, h is the uniform transverse magnetic field and Δ denotes the anisotropy parameter. It is clear that in the unit cell, there are four different links, two equal ferromagnetic and two non-equal antiferromagnetic links.

For $J_{AF} = 0$ and in the absence of the magnetic field, the spins on odd links form local triplets and the model reduces to the spin-1 chain. As soon as the magnetic field is applied all spins on odd links will be aligned along the magnetic field. On the other hand, in the absence of the space modulation, $\delta = 0$, the model reduces to the well-known alternating Heisenberg spin-1/2 chains in a transverse magnetic field¹². Two Ising-type quantum phase transitions in presence of the transverse magnetic field have been identified. A gapped phase named

*email: javahedi@gmail.com
Tel: (+98)9111554504
Fax: (+98)15133251506

stripe-antiferromagnetic has been found in the ground state phase diagram.

In presence of the space modulation, $\delta \neq 0$, the isotropic model ($\Delta = 1$) is known³⁸ very well (see Fig. 2 (a)). Four Ising-type quantum phase transitions happen by applying the magnetic field. In principle, compared with the bond alternating model, the space modulation in the isotropic case, induces a new gaped phase in the ground state phase diagram. By opening this new gap, a magnetization mid-plateau appears.

In this paper we study the effect of a transverse magnetic field on the ground state phase diagram of the model. First, by assuming that the antiferromagnetic couplings are dominant we show that the model can be regarded as an XYZ chain in the mutual effect of the longitudinal and staggered magnetic fields. Then, to explore the nature of the spectrum and the phase transition, we used the Lanczos method to numerically diagonalize finite chains. Using the exact diagonalization results, we calculate the gap, the magnetization, the string order parameter, and different spin correlation functions versus the transverse magnetic field. Based on the numerical results, we show that five gaped phases exist in the ground state phase diagram (see Fig. 2 (b)). Finally, we study the quantum correlations as the entanglement and the global entanglement.

In the next section, we briefly discuss the model in the strong antiferromagnetic coupling and map the model to an effective XYZ model. In Sec. III we present numerical results on the ground state phase diagram of the system. In Sec. IV the results of the entanglement study are presented. Finally, we conclude and summarize our results in Sec. V.

II. EFFECTIVE HAMILTONIAN

In the considered limiting case of the strong antiferromagnetic coupling $J_{AF} \gg J_F$ and strong magnetic field $h \simeq J_{AF}$, one can use standard procedure⁴² to map the model onto an effective spin chain Hamiltonian, which allows us to outline the symmetry aspect of the problem under consideration. Let us start from the limit of $J_F = 0$, where at $h = 0$ the system reduces to the set of noninteracting block of pairs of spins in the singlet state. At $J_{AF} \gg J_F$, the system behaves as a nearly independent block of pair spins. Indeed an individual block of pair spins is in the singlet $|S\rangle = \frac{1}{\sqrt{2}}[|\uparrow\downarrow\rangle - |\downarrow\uparrow\rangle]$ or one of the triplet states $|T_1\rangle = |\uparrow\uparrow\rangle$, $|T_0\rangle = \frac{1}{\sqrt{2}}[|\uparrow\downarrow\rangle + |\downarrow\uparrow\rangle]$ and $|T_{-1}\rangle = |\downarrow\downarrow\rangle$ with the corresponding energies which are obtained as

$$\begin{aligned} E(S) &= -\frac{3}{4}J_{AF}, & E(T_0) &= \frac{1}{4}J_{AF}, \\ E(T_1) &= \frac{1}{4}J_{AF} - h, & E(T_{-1}) &= \frac{1}{4}J_{AF} + h, \end{aligned} \quad (2)$$

respectively. By applying the magnetic field, the energy of the triplet state $E(T_1)$, decreases and at $h = J_{AF}$

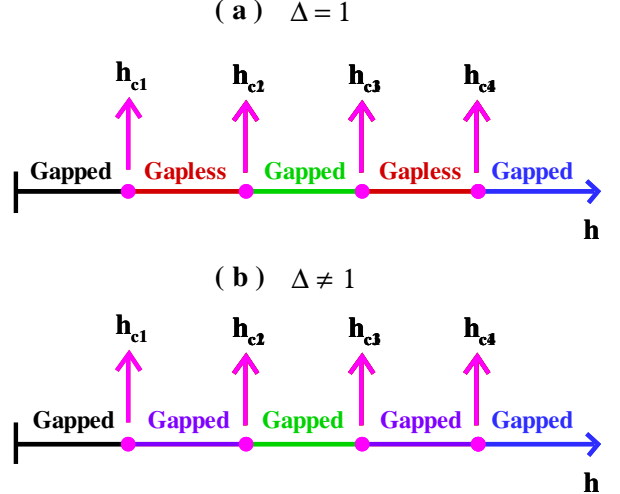


FIG. 2: (Color online) The phase diagram of the alternating tetrameric spin-1/2 chain in a transverse magnetic field: (a) Isotropic case, $\Delta = 1$, (b) Anisotropic case, $\Delta \neq 1$. Important difference is the replacing of the gapless phases of the isotropic case with gaped phases in the anisotropic case.

forms together with the singlet state a doublet of almost degenerate state. Therefore, the singlet $|S\rangle$ and the triplet $|T_1\rangle$ states construct a new subspace for an effective spin $\tau = 1/2$ system. One can project the original Hamiltonian Eq. (1) on the new singlet-triplet subspace

$$|\Downarrow\rangle \equiv |S\rangle = \frac{1}{\sqrt{2}}[|\uparrow\downarrow\rangle - |\downarrow\uparrow\rangle], \quad |\Uparrow\rangle \equiv |T_1\rangle = |\uparrow\uparrow\rangle. \quad (3)$$

The relation between the real spin operator \mathbf{S}_j and the pseudo-spin operator τ in this restricted subspace can be easily derived to the first order and up to a constant, we easily obtain the effective Hamiltonian as

$$\begin{aligned} H^{eff} &= -\frac{J_F}{2} \sum_{j=1,1}^{N/2} \left[\Delta \tau_j^x \tau_{j+1}^x + \tau_j^y \tau_{j+1}^y + \frac{1}{2} \tau_j^z \tau_{j+1}^z \right] \\ &\quad - h_0^{eff} \sum_{j=1}^{N/2} \tau_j^z - h_1^{eff} \sum_{j=1}^{N/2} \tau_j^z (-1)^j, \end{aligned} \quad (4)$$

where $h_0^{eff} = h - J_{AF} + \frac{J_F}{4}$ and $h_1^{eff} = \delta J_{AF}$. Note that in deriving (4), we have used the rotation in the effective spin space which interchanges the x and z axes. At $\Delta = 1$, the effective Hamiltonian is nothing but the XXZ Heisenberg chain in the presence of the uniform and staggered longitudinal magnetic fields⁴³⁻⁴⁵. In addition, at $\Delta = \frac{1}{2}$, the effective model is known as the XXZ model in transverse uniform and staggered magnetic fields⁴⁶. Away from the isotropic point, the effective Hamiltonian describes the fully anisotropic ferromagnetic XYZ chain in a space modulated magnetic field.

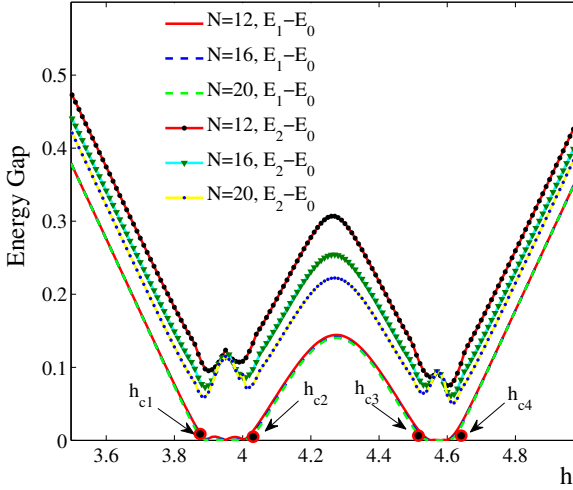


FIG. 3: (Color online). Difference between the energy of the two lowest levels as a function of the magnetic field h , for chains with exchanges $J_F = 1.0, J_{AF} = \frac{9}{2}, \delta = \frac{1}{9}$ and lengths $N = 12, 16, 20$ and $\Delta = 0.5$. The three lines for $E_1 - E_0$ are distinguishable on this scale.

III. NUMERICAL RESULTS

In this section, to explore the nature of the spectrum and the quantum phase transition, we used the Lanczos method to diagonalize numerically finite chains with lengths $N = 12, 16, 20, 24$. To get the energies of the few lowest eigenstates we considered chains with periodic boundary conditions. We start our consideration by the anisotropic case, $\Delta \neq 1$. First, we have computed the three lowest energy eigenvalues of chains with $J_F = 1.0, J_{AF} = \frac{9}{2}, \delta = \frac{1}{9}$ and different values of the anisotropy parameter $\Delta = 0.25, 0.5, 0.75$. In Fig. 3, we have plotted results of these calculations for the anisotropy parameter $\Delta = 0.5$. It can be seen that, in the absence of the magnetic field, the spectrum of the model is gapful. As soon as the magnetic field is applied, the energy of excited states decreases linearly and vanishes (N goes to infinity) at h_{c1} , which is size independent. We define the energy gap as a difference between the second excited energy and the ground state energy. By more increasing the magnetic field, the energy gap which appears at $h > h_{c1}$ first increases, then starts to decrease and again vanishes at h_{c2} . With the continuing increase in the magnetic field, the similar incident repeated twice. In principle, there are five gapped phases in the ground state phase diagram of the system which are separated by four critical fields,

$$\begin{aligned} h_{c1} &= 3.86 \pm 0.01, \\ h_{c2} &= 4.01 \pm 0.01, \\ h_{c3} &= 4.53 \pm 0.01, \\ h_{c4} &= 4.61 \pm 0.01. \end{aligned} \quad (5)$$

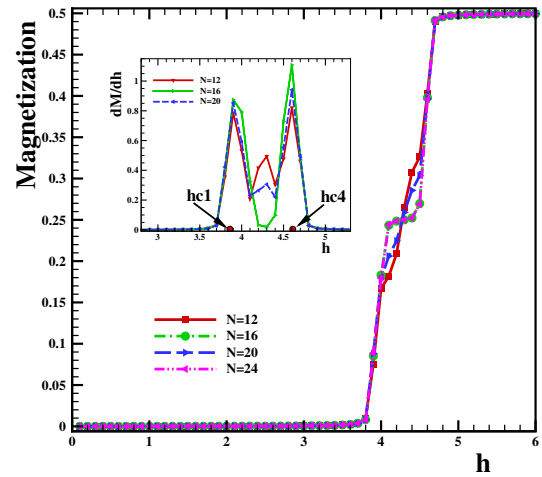


FIG. 4: (Color online.) The magnetization along the magnetic field M^x as function of applied field h , for chains with exchanges $J_F = 1.0, J_{AF} = \frac{9}{2}, \delta = \frac{1}{9}$ and lengths $N = 12, 16, 20, 24$ and $\Delta = 0.5$. The inset has shown the first derivative of the magnetization.

It should be noted, that only in two gapped phases: (I) $h_{c1} < h < h_{c2}$, (II) $h_{c3} < h < h_{c4}$ the ground state energy is doubly degenerate. In the region $h > h_{c2}$, the gap becomes proportional to h . Here, we should address that the mechanism of the opening gap is due to the alternation of a spin-1/2 chain in the region $h < h_{c1}$, the anisotropy on the FM exchanges in the regions $h_{c1} < h < h_{c2}, h_{c3} < h < h_{c4}$, the space-modulation on the AF exchanges in the region $h_{c2} < h < h_{c3}$, and the magnetic field in the saturated region $h > h_{c4}$.

To recognize the different phases induced by the transverse magnetic field in the ground state phase diagram, we have implemented the Lanczos algorithm and calculated the lowest eigenstates, the order parameter and various spin-spin correlation functions. A deep insight into the nature of the different phases can be obtained by studying the magnetization process. The magnetization along the transverse magnetic field axis is defined as

$$M^x = \frac{1}{N} \sum_{n=1}^N \langle Gs | S_n^x | Gs \rangle, \quad (6)$$

where the notation $\langle Gs | \dots | Gs \rangle$ represents the expectation value at the ground state. In Fig. 4, we have plotted M^x as a function of the magnetic field h . For arriving at this plot we considered exchange parameters $J_F = 1.0, J_{AF} = \frac{9}{2}, \delta = \frac{1}{9}$ and anisotropy parameter $\Delta = 0.5$. The standard singlet and saturated ferromagnetic plateaus at $h < h_{c1}$ and $h > h_{c2}$ are observed. Due to the profound effect of the quantum fluctuations, the transverse magnetization remains small but finite for $0 < h < h_{c1}$ and reaches zero at $h = 0$. This behavior is in agreement with expectations, based on general state-

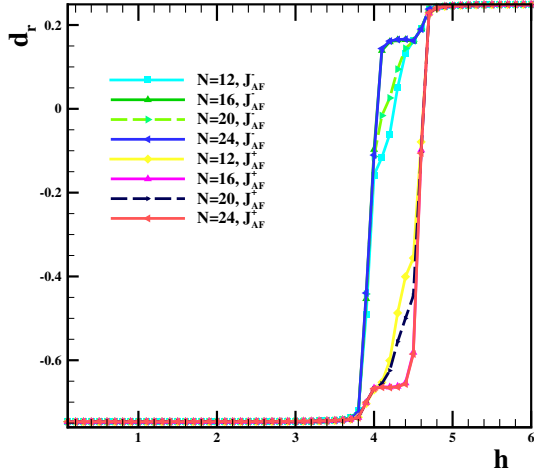


FIG. 5: (Color online). The *AF*-bond dimerization order parameter as a function of the applied field h , for chain with exchanges $J_F = 1.0, J_{AF} = \frac{9}{2}, \delta = \frac{1}{9}$ and lengths $N = 12, 16, 20, 24$.

ment that in a gapped phase, the magnetization along the applied field appears only at a finite critical value of the magnetic field equal to the energy gap. By more increasing the magnetic field, magnetization increases for $h > h_{c1}$ very fast. However, in finite size systems we do not observe a sharp transition close to the saturation value, which happens at $h > h_{c4}$. The values of the critical fields h_{c1} and h_{c4} depend on the anisotropy parameter Δ . By increasing Δ , the critical fields take larger values. Also, our numerical results show that the magnetizations along the directions perpendicular to the applied field, M^y and M^z remain zero. Critical fields can be also determined from the anomalies in the first derivation of some physical functions such as the magnetization versus h . The inset of Fig. 4 shows $\frac{dM}{dh}$ as a function of the magnetic field for different chain sizes $N = 12, 16, 20$. As it is seen, the critical fields $h_{c1} = 3.86 \pm 0.01$ and $h_{c4} = 4.61 \pm 0.01$ are determined from anomalies in the first derivation of the magnetization with respect to the h . To get additional insight into the nature of different phases, we have also calculated the bond dimerization order parameter d_r . We define the antiferromagnetic bond dimerization as

$$d_r^w = \frac{4}{N} \sum_{j=1}^{N/2} \langle Gs | S_{2j-1} \cdot S_{2j} | Gs \rangle, \\ d_r^s = \frac{4}{N} \sum_{j=2}^{N/2} \langle Gs | S_{2j-1} \cdot S_{2j} | Gs \rangle, \quad (7)$$

taking sum over antiferromagnetic weak (odd values of j) or strong (even values of j) bond, respectively. In Fig. 5 we have plotted the d_r^w and d_r^s as a function of the mag-

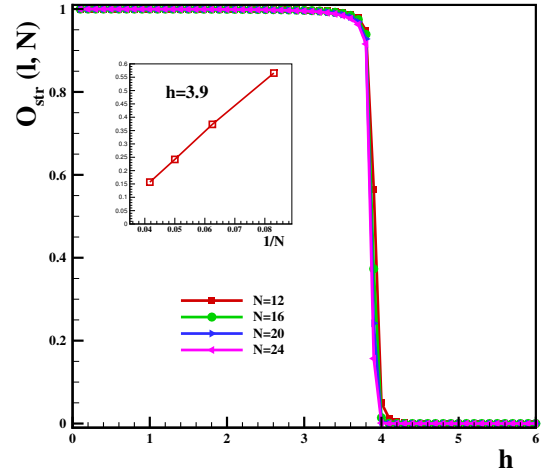


FIG. 6: (Color online). The string correlation function $O_{str}(l, N)$ as function of the transverse magnetic field h for different chain lengths $N = 12, 16, 20, 24$ with exchanges $J_F = 1.0, J_{AF} = \frac{9}{2}, \delta = \frac{1}{9}$ and $\Delta = 0.5$. The inset show the string order parameter $O_{str}(l, N)$ as function of the $1/N$ for a value of magnetic field $h = 111 > h_{c1}$.

netic field h , for chains with exchanges $J_F = 1.0, J_{AF} = \frac{9}{2}, \delta = \frac{1}{9}$ and $\Delta = 0.5$. At the first glance, it is seen that in the region $h < h_{c1}$ pair of spins on all antiferromagnetic bonds are in the singlet state with $d_r^w = d_r^s \simeq 0.75$, while at $h > h_{c4}$, all spins are aligned and $d_r^w = d_r^s \simeq \frac{1}{4}$. Numerical results in the intermediate region of the magnetic field, $h_{c1} < h < h_{c4}$, give us ability to trace the mechanism of singlet pair melting with respect to the field. As soon as the magnetic field increase from h_{c1} , all spin singlet pairs start to melt simultaneously. With further increase of h , melting of weak antiferromagnetic bonds gets more intensive, however at $h_{c2} < h < h_{c3}$ the process of melting are suppressed. As it is seen in Fig. 5 weak antiferromagnetic bonds are suppressed, however their dimerization is far from the saturation value, while the strong antiferromagnetic bonds still manifest strong singlet features. In the region $h > h_{c3}$, antiferromagnetic bonds starts to melt more intensively while weak antiferromagnetic bonds increase slowly. Finally at $h > h_{c4}$ both subsystems of antiferromagnetic bonds achieve an identical almost fully polarized state.

By analyzing of the numerical results on the energy gap (Fig. 3), we found that the spectrum is gapful in the absence of the uniform transverse magnetic field which is one of the properties of the Haldane phase with long-range string order⁴⁷. The Haldane phase can be recognized from studying the string correlation function. The string correlation function in a chain of length N defined

only for odd l as⁴⁸

$$\mathbf{O}_{str}(l, N) = -\langle \exp\{i\pi \sum_{k=2j+1}^{2j+1+l} (S_k^z)\} \rangle. \quad (8)$$

In particular, we have calculated the string correlation function for different finite chain lengths. (Since the present model has a $SU(2)$ symmetry in the absence of the magnetic field, we only consider the Z component of the string correlation function.) In Fig. 6, we have plotted $\mathbf{O}_{str}(l, N)$ as a function of the magnetic field h for different values of the chain lengths $N = 12, 16, 20, 24$ with exchanges $J_F = 1.0, J_{AF} = \frac{9}{2}, \delta = \frac{1}{9}$ and $\Delta = 0.5$. As can be seen from this figure, at $h < h_{c_1}$, $\mathbf{O}_{str}(l, N)$ is close to its maximum value 1.0, therefore the tetrameric chain system is in the Haldane phase. The Haldane phase remains stable even in the presence of a transverse magnetic field less than h_{c_1} . In the inset of the Fig. 6, we have also plotted the string order parameter, $\mathbf{O}_{str}(l, N)$, as a function of $1/N$ for a value of magnetic field $h > h_{c_1}$. It is clear that by increasing the size of the system, the $\mathbf{O}_{str}(l, N)$, converges to very small values close to zero, which shows that there is not the string ordering at larger values of the transverse magnetic field $h > h_{c_1}$.

IV. ENTANGLEMENT STUDY

The quantum correlation, which known as entanglement is a purely quantum phenomenon with no classical counterpart. It is thought to hold the key to a deeper understanding of the theoretical aspects of quantum mechanics. It has been found that entanglement⁴⁹ plays a crucial role in the low-temperature physics of many of these systems, particularly in their ground (zero temperature) state^{50–53}. In recent studies of many thermodynamic systems exhibiting (Quantum Phase Transition) QPT, in particular quantum spin models^{50–53}, it has become clear that the onset of transition is accompanied by a marked change in the entanglement. Depending on the model, entanglement could peak, or show discontinuous behavior, or show diverging derivatives with scaling behavior at the critical point⁵⁴.

A. CONCURRENCE

In this section we focus on entanglement between two sites which is known as the concurrence. We compute the entanglement of two spins in different phases of the system, which allows us to verify the melting process. Concurrence is a measure of the bipartite entanglement which is defined as following^{49,54}

$$C_{lm} = 2 \max\{0, C_{lm}^{(1)}, C_{lm}^{(2)}\},$$

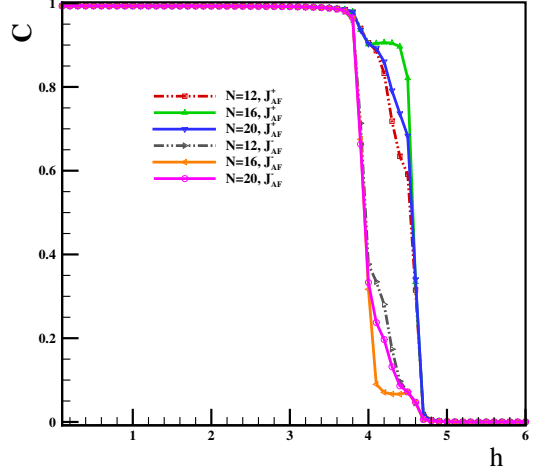


FIG. 7: (Color online). (a)The concurrence between two spins on strong J_{AF}^+ and weak J_{AF}^- links as a function of magnetic field versus applied magnetic field for chain with different lengths $N = 12, 16, 20, 24$, exchange parameter $J_F = 1.0$, $J_{AF} = \frac{9}{2}$, $\delta = \frac{1}{9}$ and anisotropy parameter $\Delta = 0.5$.

where

$$\begin{aligned} C_{lm}^{(1)} &= \sqrt{(g_{lm}^{xx} - g_{lm}^{yy})^2 + (g_{lm}^{xy} + g_{lm}^{yx})^2} \\ &- \sqrt{\left(\frac{1}{4} - g_{lm}^{zz}\right)^2 - \left(\frac{M_l^z - M_m^z}{2}\right)^2} \\ C_{lm}^{(2)} &= \sqrt{(g_{lm}^{xx} + g_{lm}^{yy})^2 + (g_{lm}^{xy} - g_{lm}^{yx})^2} \\ &- \sqrt{\left(\frac{1}{4} + g_{lm}^{zz}\right)^2 - \left(\frac{M_l^z + M_m^z}{2}\right)^2}. \end{aligned} \quad (9)$$

and $g_{lm}^{\alpha\beta} = \langle S_l^\alpha S_m^\beta \rangle$ is the correlation function between spins on sites l and m . In the region $h < h_{c_1}$, where the system is in the non-magnetic singlet phase, the correlations g^{xx}, g^{yy}, g^{zz} are the same and take the value $-1/4$. Therefore the concurrence becomes one. On the other hand, for very large values of the magnetic field, $h > h_{c_4}$, the ground state of the system is written as

$$|Gs\rangle = |\uparrow\uparrow\uparrow\ldots\uparrow\rangle. \quad (10)$$

In this saturated ferromagnetic phase, the value of correlations are $g^{xx} = g^{yy} = 0$, $g^{zz} = 1/4$ and $M^z = 1/2$ and the concurrence vanishes. It can be seen that the numerical results, are in well agreement with what is expected. In principle our numerical experiment shows that in the absence of the magnetic field, spins are completely entangled. .

We have plotted the entanglement of two spins which are located at the same strong or weak bond versus h with different chain lengths $N = 12, 16, 20, 24$ and exchange parameter $J_F = 1.0$, $J_{AF} = \frac{9}{2}$, $\delta = \frac{1}{9}$ and anisotropy parameter $\Delta = 0.5$. Fig. 9 shows the concurrence between two spins on strong J_{AF}^+ and weak J_{AF}^- links as

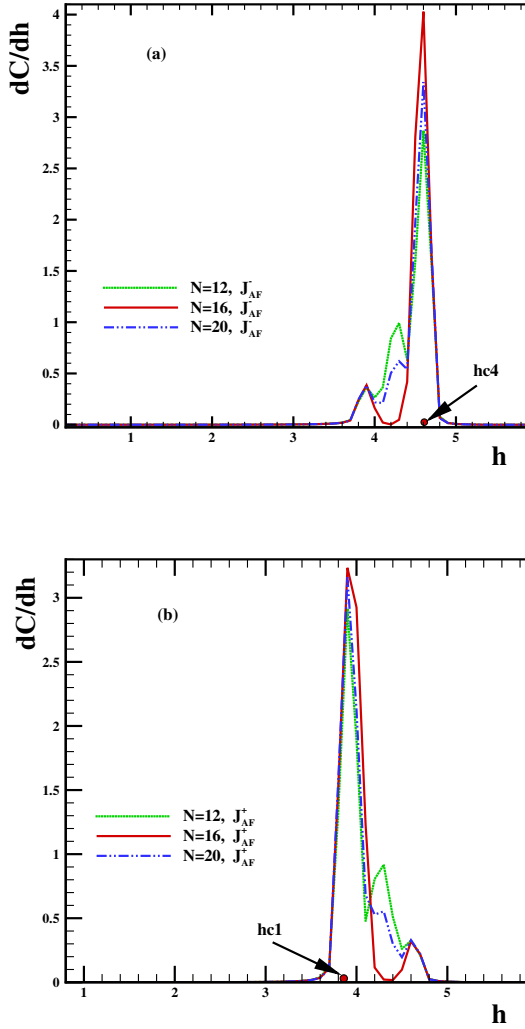


FIG. 8: (Color online). The first derivation of the concurrence between two spins on (a) weak AF_1 and (b) strong AF_2 links respectively, as a function of magnetic field for chain with exchange parameter $J_F = 1.0$, $J_{AF} = \frac{9}{2}$, $\delta = \frac{1}{9}$ and anisotropy parameter $\Delta = 0.5$.

a function of magnetic field. It is clear that in the absence of the magnetic field, pair spins on weak and strong antiferromagnetic bonds are maximally entangled.

Increasing of the magnetic field does not make change on the entanglement between pair spins on strong and weak antiferromagnetic bonds up to the first critical field h_{c1} . This behavior is in agreement that in the gapped singlet phase, the change in any physical function appears only at a critical value of the magnetic field equal to the gap. For $h > h_{c1}$ the concurrence between spins on weak bonds J_{AF}^- drops very rapidly when compared with strong exchanges J_{AF}^+ . Indeed, the quantum correlations of the two spins with strong and weak antiferromagnetic exchanges decrease with increasing the magnetic field,

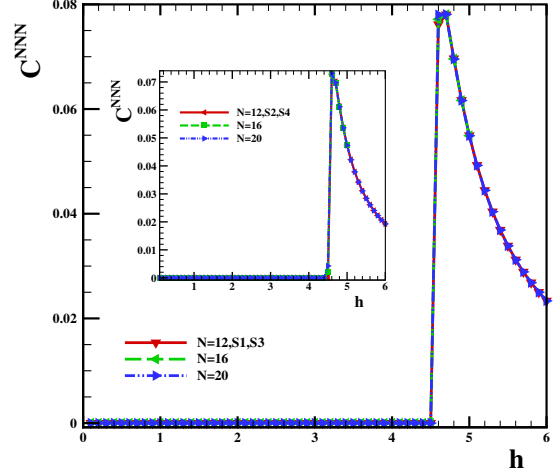


FIG. 9: (Color online). The concurrence between next nearest neighbors (NNN) spins as a function of h for chains with exchanges $J_F = 1.0$, $J_{AF} = \frac{9}{2}$, $\delta = \frac{1}{9}$ and lengths $N = 12, 16, 20$ and $\Delta = 0.5$.

but with the different intensity. In fact, such a intense quantum fluctuations cause to change in any physical function in the intermediate region. In the intermediate region the decreasing behavior of the concurrence continues up to the fourth critical field h_{c4} , where takes the zero value. Finally, in the full-saturated ferromagnetic state, all of concurrence disappears and the entanglement of the state is exactly zero.

Fig. 8 shows the derivative of the concurrence with respect to the field, $\frac{dC}{dh}$, for weak J_{AF}^- and strong J_{AF}^+ links a function of the magnetic field for different chain size $N = 12, 16, 20$, respectively. As can be clearly seen, the critical fields are $h_{c1} = 3.86 \pm 0.01$ (bottom panel) and $h_{c4} = 4.61 \pm 0.01$ (top panel) from the anomalies in the first derivation of the concurrence curve as a function of h .

To get more information about the entanglement between spins, we have also calculated the concurrence between next nearest neighbor (NNN) pair spins in the system. In Fig. 9, we have depicted the concurrence between NNN pair spins on the odd and even site as a function of h . It is obvious that the NNN pair spins are not entangled at $h = 0$. It is also remarkable that from our numerical results we found that the concurrence between NNN is zero up to h_{c3} . In the presence of the magnetic field the NNN pair spins will be entangled only in the region $h_{c3} < h < h_{c4}$. It shows very sharp response to the applied magnetic field at the critical value h_{c4} . Moreover, by increasing the magnetic field the concurrence between NNN pair spins starts to decrease monotonically.

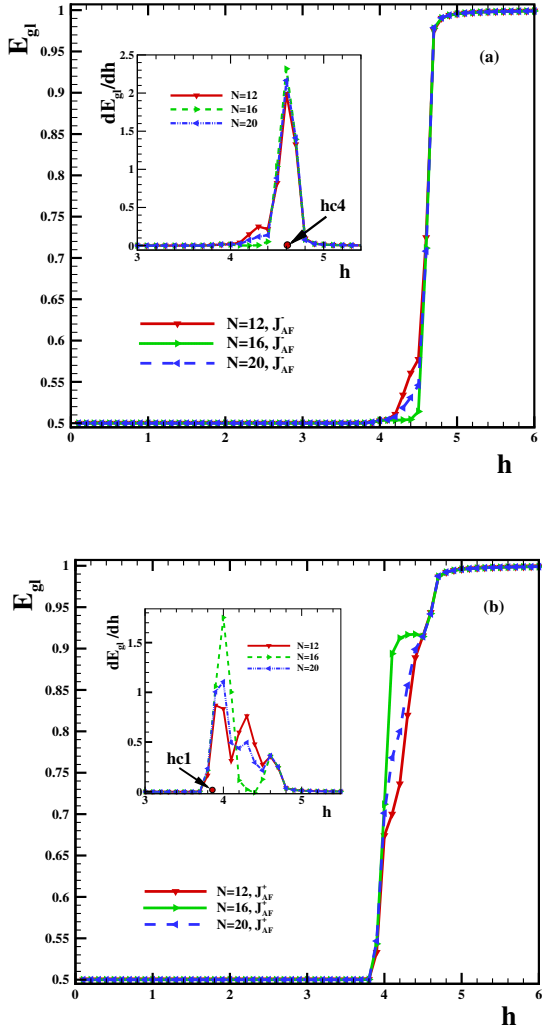


FIG. 10: (Color online). The global entanglement on (a) weak AF_1 and (b) strong AF_2 links respectively, as a function of h for chains with exchanges $J_F = 1.0, J_{AF} = \frac{9}{2}, \delta = \frac{1}{9}$ and lengths $N = 12, 16, 20$ and $\Delta = 0.5$.

B. Global entanglement

Global-entanglement (E_{gl}), offered by Meyer and Wallach⁵⁵, measures the per particle total nonlocal information in a general multipartite system^{56,57}

$$E_{gl} = \frac{1}{N} [2 \sum_{i_1 < i_2} \tau_{i_1 i_2} + \dots + N \sum_{i_1 < \dots < i_N} \tau_{i_1 \dots i_N}], \quad (11)$$

here E_{gl} is the average of tangles scaled with the total number of particles ($\frac{\langle \tau \rangle}{N}$), without extensive knowledge of tangle distribution among the each particles. Therefore, E_{gl} is an average quantity and cannot recognize between entangled states that have equal tangle but different distributions of $\langle \tau \rangle$. To get more intuition, we have computed numerically the Global en-

tanglement between spins. In Fig. 10 we have plotted Global entanglement of the same strong, weak bond as a function of the magnetic field for chains with exchanges $J_F = 1.0, J_{AF} = \frac{9}{2}, \delta = \frac{1}{9}$ and lengths $N = 12, 16, 20$ and $\Delta = 0.5$.

The general behavior comes out from E_{gl} is clear that it shows a reverse trend in comparison with the concurrence. Indeed, one can expect such behavior in which for maximal two parties entanglement there is not left any information to share among other parties. So the E_{gl} is exactly zero for the region ($h < h_{c1}$) which the concurrence is maximum. On the contrary, in the region ($h > h_{c4}$) where the concurrence is zero, the E_{gl} reaches its maximum value. It signals for the region, which entanglement between two parties is totally absent, the amount of entanglement which is shared between other entities is maximum. However, for $h > h_{c4}$ system lives in the saturated ferromagnetic phase, but one can see the global entanglement shared on strong and weak antiferromagnetic links is maximum. Moreover, in the intermediate region for $h_{c1} < h < h_{c4}$, the E_{gl} finds value, but its amount is different for weak and strong links. Indeed, by increasing magnetic field the E_{gl} shared among the weak links J_{AF}^- starts to increase very sharply at h_{c4} (see the inset of Fig. 10 (a)) while the E_{gl} shared among the strong links J_{AF}^+ starts at h_{c1} (see the inset of Fig. 10 (b)).

V. CONCLUSION

In this paper, we have studied the ground state phase diagram of the antiferromagnetic dominant ($J_{AF} >> J_F$) tetrameric spin-1/2 chain with anisotropic ferromagnetic coupling in a transverse magnetic field h . In the limit where the antiferromagnetic coupling is dominant $J_{AF} >> J_F$ we have mapped the model (1), onto an effective XYZ Heisenberg chain in an external effective field h^{eff} . This mapping allowed us to relate the isotropic case $\Delta = 1$. Using the accurate Lanczos method of numerically diagonalization for chains up to $N = 24$, we have studied the effects of an external magnetic field on the ground state properties of the system. Using the exact diagonalization results, we have calculated the various order parameter as a function of the transverse magnetic field.

In the first part of the numerical experiment, we have investigated the energy gap of the system. In the second part of the numerical experiment, we have studied the magnetization. We also calculate the string correlation function and bond-dimer order parameters. By studying the string correlation function, we found that in the absence of the magnetic field, the suggested alternating chain is in dimer (Haldane) phase and this phase remains stable in the presence external magnetic field up to the first critical field. In principle, we have addressed five gapped phases in the ground state phase diagram of the system which are separated by four crit-

ical fields, $h_{c_1} = 3.86 \pm 0.01$, $h_{c_2} = 4.01 \pm 0.01$, $h_{c_3} = 4.53 \pm 0.01$, $h_{c_4} = 4.61 \pm 0.01$.

To get more physical insight we have also investigated the concurrence and global-entanglement between spins as a function of the magnetic field. Both quantities show

the occurrence of quantum phase transitions and the corresponding critical points. It is also worth noting that the concurrence and global-entanglement show different trend in each mentioned phases.

¹ Sabir Sachdev, "Quantum phase transitions" Cambridge University Press. ISBN 0-521-00454-3, (2001).

² S. Takada, J. Phys. Soc. Japan **61**, 428 (1992).

³ K. Hida, S. Takada, J. Phys. Soc. Japan **61**, 1879 (1992); K. Hida, Phys. Rev. B **46**, 8268 1992; K. Hida, Phys. Rev. B **45**, 2207 (1992); K. Hida, J. Phys. Soc. Japan **62**, 439 (1993); K. Hida, J. Phys. Soc. Japan **63**, 2514 (1994).

⁴ M. Kohmoto, H. Tasaki Phys. Rev. B **46** 3486 (1992).

⁵ M. Yamanaka, Y. Hatsugai, M. Kohmoto Phys. Rev. B **48**, 9555 (1993).

⁶ T. Sakai, J. Phys. Soc. Japan **64**, 251 (1995).

⁷ G. S. Uhrig, H. J. Schulz, Phys. Rev. B **54**, R9624 (1996).

⁸ T. Barnes, J. Riera, D. A. Tennant, Phys. Rev. B **59**, 11384 (1999).

⁹ M. Bocquet, T. Jolicoeur, Eur. Phys. J. B **14**, 47 (2000).

¹⁰ S. Yamamoto, K. Funase, Low Temp. Phys. **31**, 740 (2005).

¹¹ W. Zheng, C. J. Hamer and R. R. P. Singh, Phys. Rev. B **74**, 172407 (2006).

¹² S. Mahdavifar and A. Akbari, J. Phys. Soc. Japan **77**, 024710 (2008).

¹³ J. Abouie and S. Mahdavifar, Phys. Rev. B **78**, 184437 (2008).

¹⁴ G. Q. Zhong, S. S. Gong, Q. R. Zheng, G. Su, Physics Letters A **373**, 1687 (2009).

¹⁵ M. Schmitt, O. Janson, S. Golbs, M. Schmidt, W. Schnelle, J. Richter, H. Rosner, Phys. Rev. B **89**, 174403 (2014).

¹⁶ G. H Liu, W. Li, G. Su, G. S Tian, The European Physical Journal B **87**, 105 (2014).

¹⁷ B. Willenberg, H. Ryll, K. Kiefer, D. A. Tennant, F. Groitl, K. Rolfs, P. Manuel, D. Khalyavin, K. C. Rule, A. U. B. Wolter, and S. Süllow, Phys. Rev. B **91**, 060407(R) (2015).

¹⁸ Yu-Chin Tzeng, Li Dai, Ming-Chiang Chung, Luigi Amico, Leong-Chuan Kwek, Scientific Reports **6**, 26453 (2016).

¹⁹ M. Hagiwara, Y. Narumi, K. Kindo, T. C. Kobayashi, H. Yamakage, K. Amaya and G. Schumauch J. Phys. Soc. Japan **66**, 1792 (1997).

²⁰ M. Takahashi, Y. Hosokoshi, H. Nakano, T. Goto, M. Kinoshita, Mol. Cryst. Liq. Crist. Sci. Technol. Sec. A **306**, 111 (1997).

²¹ B. Lake, R. A. Cowley, D. A. Tennant J. Phys.: Cond. Matt. **9**, 10951 (2000); A. W. Garrett, S. E. Nagler, D. A. Tennant, B. C. Sales, T. Barnes Phys. Rev. Lett. **79**, 745 (1997).

²² H. Manaka, I. Yamada, K. Yamaguchi J. Phys. Soc. Japan **66**, 564 (1997).

²³ H. Manaka, I. Yamada, J. Phys. Soc. Japan **66**, 1908 (1997).

²⁴ K. Kodama, H. Harashina, H. Sakai, M. Kato, M. Sato, K. Kakurai, M. Nishi, J. Phys. Soc. Japan **68**, 237 (1999).

²⁵ G. Xu, C. Broholm, D. H. Reich, M. A. Adams, Phys. Rev. Lett. **84**, 4465 (2000).

²⁶ Y. Inagaki, A. Kobayashi, T. Asano, T. Sakon, H. Kitagawa, M. Motokawa, Y. Ajiro, J. Phys. Soc. Japan **74**, 2683 (2005).

²⁷ M. B. Stone, W. Tian, M. D. Lumsden, G. E. Granroth, D. Mandrus, J. H. Chung, N. Harrison, S. E. Nagler Phys. Rev. Lett. **99**, 087204 (2007).

²⁸ M. B. Stone, Y. Chen, D. H. Reich, C. Broholm, G. Xu, J. R. D. Copley, and J. C. Cook, Phys. Rev. B **90**, 094419 (2014).

²⁹ H. Yamaguchi, Y. Shimpuku, T. Shimokawa, K. Iwase, T. Ono, Y. Kono, S. Kittaka, T. Sakakibara, Y. Hosokoshi, Phys. Rev. B **91**, 085117 (2015).

³⁰ Y. Ajiro, T. Asano, T. Inami, H. Aruga-Katori and T. Goto, J. Phys. Soc. Japan **63**, 859 (1994).

³¹ K. Hida, J. Phys. Soc. Japan **63**, 2359 (1994).

³² K. Okamoto, Solid State Commun. **98**, 245 (1996).

³³ A. Escuer, R. Vicente, M. S. El Fallah, M. A. S. Goher and F. A. Mautner, Inorg. Chem. **37**, 4466 (1998).

³⁴ H. T. Lu, Y. H. Su, L. Q. Sun, J. Chang, C. S. Liu, H. G. Luo, and T. Iang, Phys. Rev. B **71**, 144426 (2005).

³⁵ Bo Gu, Gang Su and Song Gao, Phys. Rev. B **73**, 134427 (2006).

³⁶ Shou-Shu Gong, Bo Gu and Gang Su, Phys. Lett. A **372**, 2322 (2008).

³⁷ Shou-Shu Gong, Gao Song and Gang Su, Phys. Rev. B **80**, 014413 (2009).

³⁸ S. Mahdavifar, J. Abouie, J. Phys.: Cond. Matt. **23**, 246002 (2011).

³⁹ M. Shahri Naseri, G. I. Japaridze, S. Mahdavifar, S. Farjam Shavesteh, J. Phys.: Cond. Matt. **24**, 116002 (2012).

⁴⁰ M. Shahri Naseri, G. I. Japaridze, S. Mahdavifar, S. Farjam Shavesteh, physica status solidi (b) **250**, 338 (2012).

⁴¹ Zhang Kai-Cheng, GS Tian and Chi Feng, Communications in Theoretical Physics **61**, 263 (2013).

⁴² F. Mila, Eur. Phys. J. B **6**, 201 (1998).

⁴³ F. C. Alcaraz, A. L. Malvezzi, J. Phys. A: Math Gen **28**, 1521 (1995).

⁴⁴ J. Lou, et al., Phys. Rev. Lett. **94**, 217207 (2005).

⁴⁵ S. Mahdavifar, Eur. Phys. J. B **55**, 371 (2007).

⁴⁶ H. Moradmard, M. Shahri Naseri, S. Mahdavifar, J. Supercond. Nov. Magn. **27**, 1265 (2014).

⁴⁷ F. D. M. Haldane, Phys. Rev. Lett **50**, 1153 (1983).

⁴⁸ K. Hida: Phys. Rev. Lett. **83**, 3297 (1999).

⁴⁹ W. K. Wootters, Phys. Rev. Lett. **80**, 2245 (1998).

⁵⁰ T. J. Osborne, M. A. Nielsen, Phys. Rev. A **66**, 032110 (2002).

⁵¹ A. Osterloh, L. Amico, G. Falci, and R. Fazio, Nature **416**, 608 (2002).

⁵² G. Vidal, J. I. Latorre, E. Rico, and A. Kitaev, Phys. Rev. Lett. **90**, 227902 (2003).

⁵³ P. Lou and J.Y. Lee, Phys. Rev. B **74**, 134402 (2006).

⁵⁴ L. Amico, R. Fazio, A. Osterloh, and V. Vedral, Rev. Mod. Phys. **80**, 517 (2008).

⁵⁵ D. A. Meyer and N. R. Wallach, J. Math. Phys. **43**, 4273 (2002).

⁵⁶ G. K. Brennen, Quant. Inf. and Comput. **3**, 616 (2003).

⁵⁷ J. Vahedi, M. R. Soltani and S. Mahdavifar, J. Supercond.

